Correction of Head Movement on PET Studies: Comparison of Methods

Andrew J. Montgomery[1], Kris Thielemans[2], Mitul A. Mehta[1], Federico Turkheimer[2], Sanida Mustafovic[2], and Paul M. Grasby[1]

[1]CSC–MRC Cyclotron Unit, Imperial College, Hammersmith Hospital, London, United Kingdom; and [2]Hammersmith Imanet, Hammersmith Hospital, London, United Kingdom

Head movement presents a continuing problem in PET studies. Head restraint minimizes movement but is unreliable, resulting in the need to develop alternative strategies. These include frame-by-frame (FBF) realignment or use of motion tracking (MT) during the scan to realign PET acquisition data. Here we present a comparative analysis of these 2 methods of motion correction. **Methods:** Eight volunteers were examined at rest using ^{11}C-raclopride PET with the radioligand administered as a bolus followed by constant infusion to achieve steady state. Binding potential (BP) was estimated using the ratio method during 2 periods of the scan at steady state. Head movement was compensated by using coregistration between frames (FBF) and 3 methods using MT measurements of head position acquired with a commercially available optical tracking system. **Results:** All methods of realignment improved test–retest reliability and noise characteristics of the raw data, with important consequences for the power to detect small changes in radiotracer binding, and the potential to reduce false-positive and false-negative results. MT methods were superior to FBF realignment using coregistration on some indices. **Conclusion:** Such methods have considerable potential to improve the reliability of PET data with important implications for the numbers of volunteers required to test hypotheses.

Key Words: PET; ^{11}C-raclopride; movement; test–retest; striatum

J Nucl Med 2006; 47:1936–1944

Improvements in scanner resolution and increasingly ambitious attempts to measure small changes in radioligand binding mean that head movement is becoming one of the main obstacles to capitalizing on technologic advances. If movement occurs, spatial resolution is reduced (*1*), and measured signal may be either reduced or increased depending on the radioligand concentrations in areas around the defined region of interest (ROI). Thus, real differences in radioligand binding may remain undetected or, alternatively, artifactual changes may be erroneously recorded.

Various approaches to this challenge have been proposed. The most simple is to minimize head movement during the scan with head restraint. Stereotactic frames that absolutely fix the skull may be used in certain patient subgroups—for example, neurosurgical patients (*2*)—and in animal studies but generally require anesthesia because of the level of discomfort they cause. Acceptable methods for use in human studies include molded plastic masks (*1*), orthopedic collars and straps, and vacuum-lock bags (*3*). However, such methods are not able to eliminate movement entirely (*3,4*), and the more restrictive methods may be uncomfortable reducing their acceptability to volunteers, potentially giving rise to further movement to relieve discomfort.

If movement does occur during a scan, it is possible to reduce its influence by realigning the acquired PET data post hoc. Typically, this is done by realigning image frames either to an initial frame or to frames chosen because of their relatively high signal-to-noise ratio (*5*). Manipulations to improve the frame registration include denoising using wavelet filters (*5*) or using nonattenuation–corrected frames (*6*). However, these methods have several disadvantages: The quality of the registration may be limited by poor statistics, particularly in the terminal frames; the method is unable to compensate for movements that occur within frames, which may be as long as 10 min; a mismatch between the transmission and emission scans may occur, resulting in incorrect application of attenuation correction; and the redistribution of radioligand during the scan may result in artifactual realignments (*7*). An alternative approach is to place fiducial markers filled with a small quantity of radiation-emitting isotope to the scalp of the volunteer before scanning. These sources may be identified on the emission scan and used to realign the frames. This method has not been widely adopted because of potential movements between scalp and skull.

A novel approach is to measure head position during the scan and correct for any movements during the rebinning of list-mode data into sinograms, before image reconstruction (*8–11*). This method is being implemented at the CSC–MRC

Received Jan. 26, 2006; revision accepted Aug. 28, 2006.

For correspondence or reprints contact: Andrew J. Montgomery, MbBChir, PhD, CSC–MRC Cyclotron Unit, Imperial College, Hammersmith Hospital, DuCane Rd., London W12 0NN, United Kingdom.

E-mail: andrew.montgomery@imperial.ac.uk

Cyclotron Unit, Hammersmith Hospital, using a commercially available optical tracking system (Polaris; Northern Digital) (*10,12–15*). Theoretically, this method offers a superior solution to the methods based on frame-by-frame (FBF) realignment for several reasons: First, there is no mismatch to transmission scan because emission data are realigned to the position of the brain during transmission scan acquisition; second, no reliance on PET data, which may have poor spatial information, is required; and third, realignment may take place several times per second rather than relying on realignment of long frames. The system is able to significantly improve the quality of phantom data subjected to movement (*13*) but has not yet been formally assessed using PET data from studies in humans. A complementary approach is to combine motion-tracking (MT) and FBF methods by using MT recording of head position to realign frames. This method (referred to as MTfbf) allows realignment to the transmission scan position and avoids use of noisy PET data. However, head movements within frames remain uncorrected. Recently, the effect of applying motion correction to ^{18}F-altanserin parametric images has been reported (*16*). In this study, head position was recorded using Polaris and realignments were applied to individual frames. Improvements in the quality of parametric images were found, although the analysis was not quantitative. Furthermore, because realignments were applied to frames, no account could be made of within-frame movements.

In this article we directly compare methods of correction for head movement using a series of ^{11}C-raclopride scans. Single scans were acquired on resting volunteers over 100 min using a bolus followed by constant infusion (BI) administration of the radioligand. This method allows the calculation of binding potential (BP) during 2 consecutive periods of the scan (*17*). Because the scans were performed at rest and at steady state, the BP should be the same in the 2 sampling periods: Any difference in BP between these 2 periods may be assumed to be due to head movement. Other quantitative outcome measures included an assessment of the noise in the data and the rate of change of regional radioactivity.

MATERIALS AND METHODS

Volunteers

Eight volunteers, recruited for a study examining the influence of selective serotonin reuptake inhibitor antidepressants on striatal D_2 receptor binding, were included in this analysis. Five volunteers were taking antidepressants at the time of the study; 3 were healthy controls. All had been noted to move their head during emission scanning. Since comparisons reported in this article are all within-subject, the mixed population of volunteers does not present a confounder. The study was approved by the Hammersmith Hospitals Research Ethics Committee and with permission to administer the radioligand provided by the Administration of Radioactive Substances Advisory Committee, U.K. All volunteers provided written informed consent before inclusion in the studies.

PET

Scans were performed on an ECAT EXACT 3D (CPS Inc.) PET camera (5.1-mm full width half maximum resolution) (*18*). A transmission scan lasting 5 min was acquired for attenuation correction followed by the emission scan, which was acquired in list mode over 100 min. ^{11}C-Raclopride was administered as a BI with a k_{bol} = 105 min (k_{bol} represents the time for the bolus to be administered at the infusion rate) (*17*). Total administered activity was equivalent to 293 ± 54 MBq per scan, and specific radioactivity was 41,400 ± 19,700 MBq/μmol. Scans were rebinned into dynamic frame sequences (1 × variable [before radioligand injection]: 1 × 15 s, 1 × 5 s, 1 × 10 s, 1 × 30 s, 4 × 60 s, 19 × 300 s), a typical sequence for ^{11}C-radioligands receptor studies, and reconstructed both with and without attenuation correction. Sinogram normalization and dead-time and scatter correction were performed according to the procedures used in the ECAT 7.1 software distributed with the scanner. Reconstruction was performed using the 3-dimensional reprojection (3DRP) algorithm (*19*). This algorithm was chosen because it is well understood and will not introduce bias. Using iterative reconstructions for quantitative dynamic studies is a matter of ongoing research.

Head movement was minimized using a foam-lined head support with a strap over the forehead. Volunteers were asked to lie as still as possible and were not required to complete any other task during the scan.

BP was calculated for 2 periods of the scan as:

$$\mathrm{BP} = (\text{striatal counts}/\text{cerebellar counts}) - 1$$

between 38 and 53 min and 58 and 100 min. This period of sampling was designed to allow equilibrium to be established before sampling and to optimize the sensitivity of the method to detect changes in BP after a pharmacologic challenge administered (*17*) at 50 min, although in this study no challenge was used.

ROI Analysis

Dorsal and ventral striatal ROIs were defined on the single subject MR scan positioned in standard Montreal Neurologic Institute (MNI) space. The distinction between ventral and dorsal striatum was based on previously described criteria (*5*). A ^{11}C-raclopride template was constructed in MNI space (*20*). A ^{11}C-raclopride template was then spatially transformed to the individual 1- to 28-frame summated PET image within statistical parametric mapping, SPM 99 (www.fil.ion.ucl.ac.uk/spm), implemented in MATLAB version 5 (Mathworks) (*21*), and the resulting transformation parameters were used to transform the striatal ROIs into individual space. Cerebellar ROIs were defined on summated PET images (1–20 min) as 15-mm-radius circles placed manually on 5 axial planes. Time–activity curves for individual regions were generated using image analysis software (Analyze AVW 4.0; Biomedical Imaging Resource, Mayo Foundation). Activity from right and left ROIs was averaged. Separate ROIs were generated for each of the reconstructed scans.

Movement Correction Methods

FBF Realignments Without MT. The nonattenuation dynamic image was denoised using a level-2, order-64 Battle–Lemarie

wavelet (*22,23*). Frames were realigned to a single 300-s emission frame acquired 25 min after injection using a mutual information algorithm (*24*), and the transformation parameters were then applied to the corresponding attenuation-corrected dynamic image.

MT System. An optical tracking system (Polaris) used near-infrared sources to track the position of 4 reflective beads that were securely attached to a neoprene hat worn by the volunteer. Movement between the hat and the scalp was minimized by choosing the smallest hat size that the volunteer could tolerate. Head position was recorded 5 times per second. The Polaris device returns spatial information in the form of rotations in quaternion space, followed by translations in 3 dimensions, and a root-mean-square error (RMSE) on the measurement. The Polaris data were then converted to a scanner coordinate system as described by Hutton et al. (*11*), with the simplification that in our case the Polaris system was in a fixed position. To assess the effect of motion on ROI radioactivity, a composite index of motion was calculated for each Polaris time point. The RMSE was calculated by measuring the distance of 3 points in the positions of the sampled ROI (cerebellum, right and left striatum) from their position during the transmission scan. In addition, a mean RMSE for the whole scan was calculated as an index of total movement during emission scanning.

Methods Using MT. Three methods of image realignment using Polaris data were compared (Fig. 1): The first, referred to as MTfbf, is an image-based realignment method. For every frame, it repositioned the transmission image to the average position during that frame, performed the normal precorrection and reconstruction (using 3DRP) method, and finally realigned the reconstructed image to the transmission scan. In the second method, hereafter referred to as MT correction, has been described in detail by Bloomfield et al. (*13*), with enhancements to improve quantification (*14*). Lines of response (LORs), individually recorded in list mode, were realigned to the head position during the transmission scan when the list-mode data were rebinned into sinograms taking normalization factors into account. These sinograms were then postprocessed by dividing each sinogram element by the percentage of the frame duration during which the corresponding LOR was measured (i.e., fully inside the detector ring). This percentage was approximated as follows: For every time frame, 10 evenly spaced time points were taken, for which a sinogram was computed by counting the number of repositioned LORs (one for each detector pair) that contribute to every sinogram element. The average of those 10 sinograms was then divided by the equivalent sinogram obtained without motion. Note that this computation is central processing unit–intensive ($\pm$30 min per time frame on an Opteron 280 [AMD]) compared with the rebinning ($\pm$60 min for the whole scan) due to the number of detector pairs, which is about 200 million for the EXACT 3D. Attenuation correction and scatter correction were then applied to the emission data. The corrected data were then made consistent by replacing all sinogram elements that were measured for $<$30% of the frame duration by the forward projection of an initial estimate (*14*) and finally reconstructed using the 3DRP algorithm. The third method, referred to as LMCfbf (*15*) realigned all detected LORs within a frame to an average position during the frame, again taking normalization into account, repositioning the attenuation image to this average position, performing the same type of corrections and reconstruction as in the MT case and followed by moving the reconstructed image for the frame to the transmission scan position. For the MTfbf and LMCfbf methods, attenuation correction factors were derived from forward projecting an attenuation image after repositioning. The motivation for these 3 different methods is given in the Discussion.

Statistical Analysis

All values were expressed as mean $\pm$ SD. Differences across conditions were compared using repeated-measures ANOVA. Planned post hoc *t* tests were used to compare the different methods of realignment for each region (dorsal striatum [DS], ventral striatum [VS], cerebellum). Significance was set to $P < 0.05$. Stability of regional activity was calculated as the gradient of a linear least-squares fit to the ROI radioactivity between 38 and

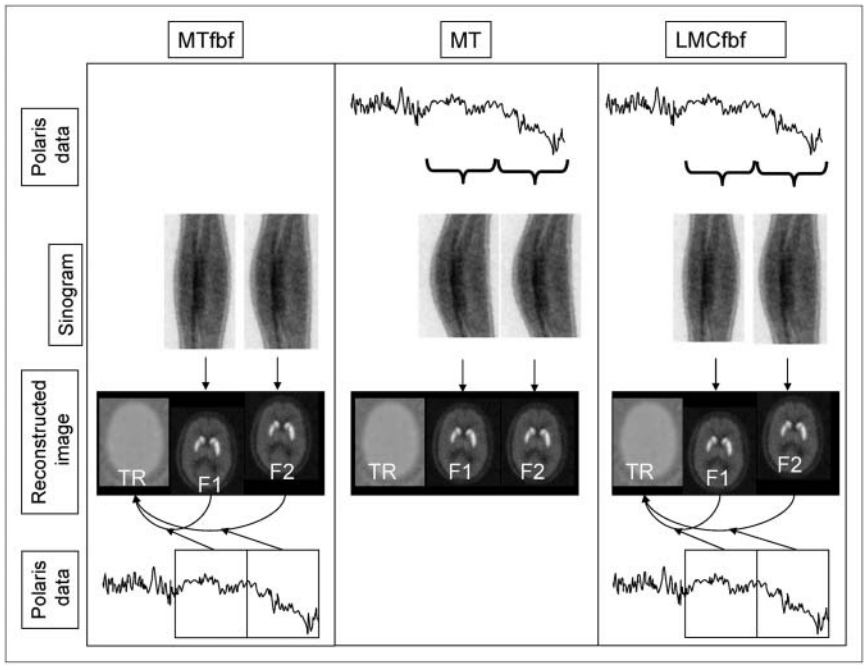

FIGURE 1. Different stages involved in realigning emission data with Polaris-based methods. MTfbf is a 1-stage process, where reconstructed frames (F1 and F2) are moved to position of the transmission scan (TR), using the average frame position derived from Polaris data. MT is a 1-stage process in which lines of response (LORs) are moved to the transmission scan position based on Polaris data. LMCfbf is a 2-stage process: First, LORs within a frame are realigned to average position in the frame using Polaris data; then reconstructed frames are moved to transmission scan position using the average frame position derived from Polaris data. For all methods, only 1 Polaris coordinate is shown for simplicity. Full details of the different methods are given in the text.

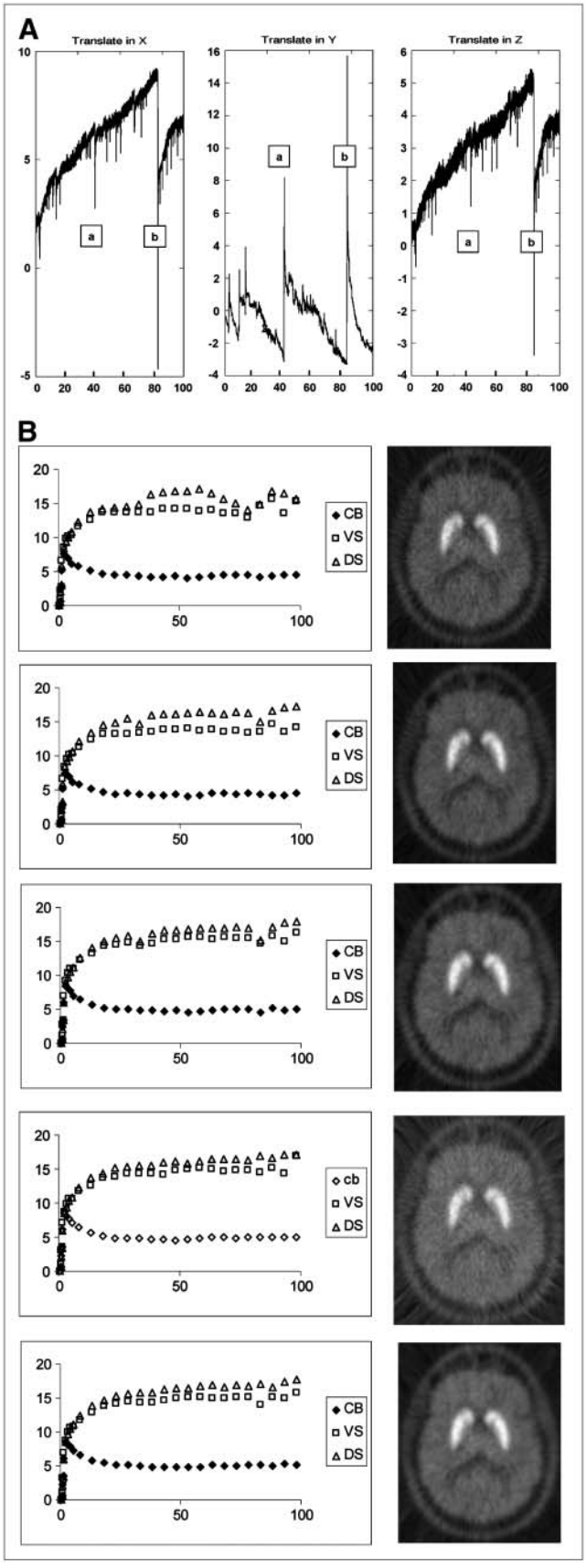

FIGURE 2. (A) Plots of Polaris translation files (X, left−right; Y, anterior/posterior; Z, dorsal/ventral): *x*-axis time = min; *y*-axis from an arbitrary starting point = mm. a and b indicate large movements. (B) Time–activity curve and PET summated images of (from top to bottom): raw PET data, FBF realignment, MTfbf realignment, MT realignment, and LMCfbf realignment. CB = cerebellum; *x*-axis time = min; *y*-axis activity = kBq/mL.

100 min and expressed as the percentage change in radioactivity per hour. Noise was assessed as the SD of the regional activities in the first and second sampling periods (38−53 min, 3 frames; 58−100 min, 8 frames) and is expressed as a percentage of the mean value (% coefficient of variance) (*5*).

Test–retest of BP values was assessed using the mean change between scans and also the absolute value of the difference between test and retest divided by the average of the test and retest values (variability). The reliability of the measurements was assessed by the intraclass correlation coefficient (ICC), calculated as:

$$\frac{\text{BSMSS} - \text{WSMSS}}{\text{BSMSS} + (\text{n}+1)\text{WSMSS}}$$

where BSMSS is between-subject mean sum of squares, WSMSS is within-subject mean sum of squares, and n is the number of observations. ICC values range from −1 (no reliability) to 1 (maximum reliability achieved when test and retest are identical).

SPM Analysis

Localized changes within the striatum may not be detected by a traditional ROI analysis; therefore, a voxel-wise comparison with SPM between the test–retest images within the striatum and across the whole brain was performed. Parametric images of BP were generated by creating images of mean activity in frames 38–53 and 58–100 min, then dividing the mean image by the respective cerebellar reference region activity and subtracting 1—that is, for each voxel, Equation 1 was applied. These images were stereotactically normalized into a standard anatomic space developed at the Montreal Neurologic Institute (MNI 152) using a reference template image provided with SPM99 (www.fil.ion.ucl.ac.uk/spm) and smoothed using an isotropic gaussian kernel of 6-mm full width at half maximum. Scans were compared using a multivariate ANOVA and presented using a statistical threshold of $P = 0.01$ (uncorrected for multiple comparisons), no spatial extent threshold, and with the analysis restricted to BP values > 1.0. Significant results are reported at $P < 0.05$ corrected for multiple comparisons (p_{corr}) across the whole brain.

RESULTS

An example of the output from Polaris and corresponding time–activity curves of the raw PET data and after different methods of head movement correction is shown in Figure 2. The pattern of movement is typical, with occasional large movements superimposed on a slow drift. The raw data time–activity curve shows greater evidence of head movement compared with the time–activity curve after movement correction. The RMSE for each individual scan is shown alongside the respective time–activity curve in Figure 3.

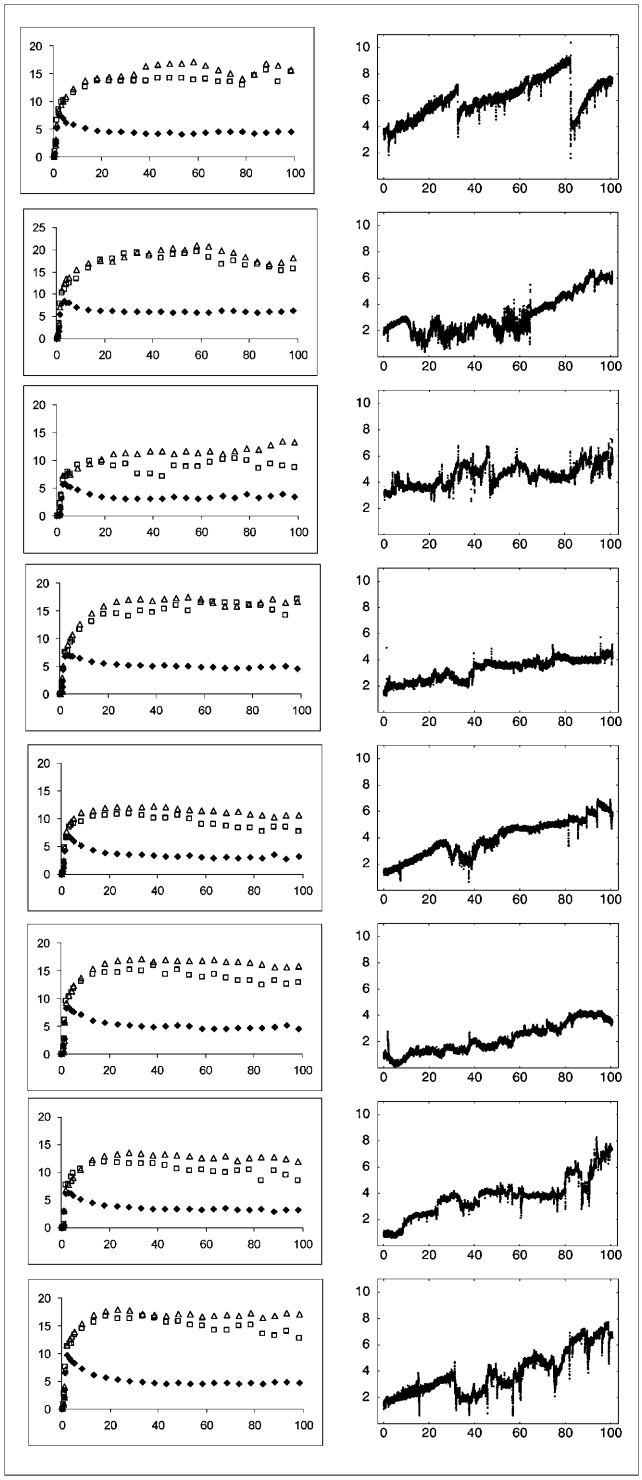

FIGURE 3. Time–activity curves (left) and RMSEs of motion (right) during scanning for each volunteer. (Left) △, DS; □, VS; ♦, cerebellum; *y*-axis = kBq/mL; *x*-axis = min. (Right) *y*-axis = mm; *x*-axis = min.

TABLE 1
Stability of Regional Activity Measured by Percentage Change in Activity per Hour

Method	Region	Mean ± SD
Raw	VS	−3.3 ± 15.9
	DS	−3.8 ± 10.1
	CB	−3.7 ± 12.5
FBF	VS	−3.3 ± 15.9
	DS	−3.2 ± 9.7
	CB	0.0 ± 8.6
MTfbf	VS	1.1 ± 10.4
	DS	1.0 ± 8.4
	CB	1.5 ± 6.6
MT	VS	−1.2 ± 14.7
	DS	−1.2 ± 7.3
	CB	1.1 ± 11.2
LMCfbf	VS*†	1.5 ± 12.9
	DS	1.1 ± 9.0
	CB	1.2 ± 8.0

*$P = 0.08$ vs. raw data.
†$P < 0.05$ compared with FBF.
CB = cerebellum.

Stability of Regional Activity Across Scanning Periods

There was no significant change of activity in any region with any of the 5 datasets (Table 1). However, ANOVA showed a significant effect of the method of realignment ($F_{4,28} = 2.95$, $P = 0.04$) with no interaction with ROI. There was a trend for a reduced rate of change of regional activity in the VS after LMCfbf compared with raw data ($t = -2.04$, $P = 0.08$) and a significant reduction after LMCfbf compared with FBF ($t = -2.54$, $P = 0.04$). No other differences were statistically significant.

Noise Levels

Noise levels in the 2 sampling periods are shown in Figure 4. As expected, noise was greater in the second sampling period ($F_{1,7} = 43.05$, $P < 0.01$), and noise varied across regions ($F_{2,14} = 9.54$, $P < 0.01$). Importantly, realignment methods reduced noise overall ($F_{4,28} = 6.28$, $P < 0.01$). Although there were no significant interactions

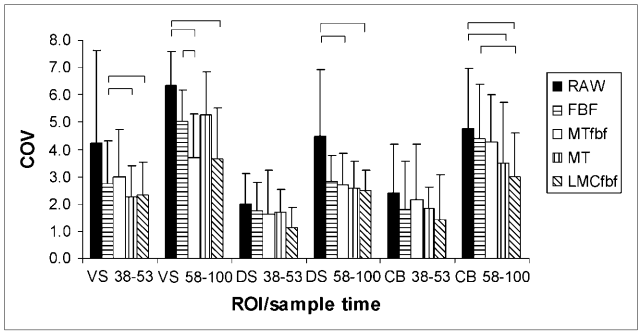

FIGURE 4. Noise levels (coefficient of variance, COV) in different regions after 5 different analyses: raw data, FBF realignment, and 3 Polaris methods (MTfbf, MT, LMCfbf). ANOVA showed significant effects of region, sample time, and method of analysis, with no interactions (error bars indicate SD; brackets indicate $P < 0.05$).

between these variables, it was important to understand the differences between methods; therefore, post hoc t tests were performed and significant differences are shown in Figure 4.

BPs

Measured BPs in the first and second sampling periods are shown for the 5 methods in Table 2 and Figure 5. ANOVA showed significant effects of region ($F_{1,7} = 60.28$, $P < 0.01$) and method of analysis ($F_{1,7} = 7.19$, $P < 0.01$) but not sample time. There were interactions between method of analysis and time ($F_{4,28} = 4.02$, $P = 0.01$) and a trend interaction between method and region ($F_{4,28} = 2.25$, $P = 0.09$). A post hoc t test showed no significant difference between the first and second sampling period in either ROI after any one method of analysis. Other comparisons are shown in (Fig. 5). There was no correlation between total RMSE motion and change in BP (data not shown).

Test–Retest Indices

Indices of test–retest reliability are shown in Table 3. ANOVA showed effects of method on variability ($F_{4,28} = 14.57$, $P < 0.01$) and region ($F_{1,7} = 8.70$, $P = 0.02$), with a significant interaction between these 2 factors ($F_{4,28} = 4.76$, $P < 0.01$). FBF ($t_7 = 5.58$, $P < 0.01$), MTfbf ($t_7 = 3.37$, $P = 0.01$), MT ($t_7 = 6.11$, $P < 0.01$), and LMCfbf ($t_7 = 5.24$, $P < 0.01$) reduced variability in the VS compared with raw data, and there was a trend reduction in the VS with MT compared with the FBF ($t = 2.24$, $P = 0.06$). There were no differences in variability in the DS. ANOVA of change showed no significant effect of method or region. The ICC in the raw data was poor in the VS (0.57) but was improved by all methods of correction for head movement, achieving values of >0.70 with all methods of realignment.

SPM Analyses

Glass brain depictions of results are shown in Figure 6. The raw data showed significant reductions in BP from period 1 to period 2 during the scan that were restricted to the anterior portions of the striatum (significant cluster peak at 26, 14, −2 (x, y, z), $t = 5.97$, $p_{corr} = 0.04$) and increases in anterior and posterior portions of the striatum (16, 6, −4, $t = 6.58$, $p_{corr} < 0.01$; −32, −16, 8, $t = 5.74$, $p_{corr} = <0.01$). No other contrasts had regions with significant differences between scanning periods when corrected for multiple comparisons.

TABLE 2
BPs in VS and DS After 5 Methods of Analysis

	VS		DS	
Method	38−53	58−100	38−53	58−100
Raw	1.92 ± 0.71	1.80 ± 0.24	2.33 ± 0.81	2.27 ± 0.23
FBF	1.92 ± 0.68	1.88 ± 0.20	2.28 ± 0.79	2.33 ± 0.17
MTfbf	1.99 ± 0.69	2.03 ± 0.13	2.33 ± 0.80	2.39 ± 0.13
MT	1.86 ± 0.24	1.85 ± 0.13	2.22 ± 0.21	2.22 ± 0.20
LMCfbf	1.94 ± 0.67	1.94 ± 0.10	2.27 ± 0.78	2.30 ± 0.14

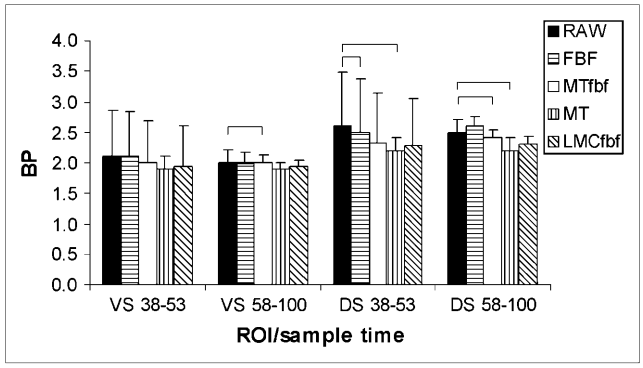

FIGURE 5. Mean BPs for VS and DS ROIs (brackets indicate paired t test, $P < 0.05$).

DISCUSSION

This article describes, to our knowledge, the first quantitative comparison on patient data between raw, FBF, and Polaris-guided methods of motion-correcting PET data. Using several different criteria and analyses, all methods of realignment were superior to the raw data with Polaris methods performing better than FBF on some indices. Using such methods, the test–retest reliability and accuracy of PET data may be dramatically improved with consequent implications for interpretation of existing results and future study design.

In the VS, all methods of motion correction improved test–retest reliability with reduced variability. The ICC in the VS was increased by all methods compared with the raw data, indicating that between-subject differences were maintained or improved by the realignment methods. The implications of these findings on the design of future studies are exemplified by consideration of their impact on power calculations: To detect a 5% difference in the VS in the raw data would require 68 volunteers (power of 0.8, $\alpha = 0.05$). The corresponding figures after the other methods are FBF, 28; MTfbf, 13; MT, 17; and LMCfbf, 14. Although studies using interventions may have different test–retest characteristics, such improvements have profound implications when considering the difficulty recruiting certain patient groups for clinical studies and the ethical issue of exposing volunteers to ionizing radiation.

All 4 methods of correction for head movement are likely to have improved the spatial accuracy of BP estimates. The degree of change in BP produced by head movements may be estimated by simulation studies in which the ROI is deliberately moved relative to the scan. For example, in the striatal subregions, small movements can cause changes in measured BP at least as large as those due to dopamine release (Fig. 7). Use of motion correction will improve the accuracy of BP measurements and enhance confidence in results, particularly in small ROIs such as the VS and DS. It is interesting to note that the changes of measured radioactivity in these 2 regions are quite different after head motion, either induced artificially, as

TABLE 3
Measures of Test–Retest Reliability for 5 Methods of Data Analysis

Method	VS			DS		
	Change	Variability	ICC	Change	Variability	ICC
Raw	−4.5 ± 14.5	13.5 ± 5.1	0.57	−2.2 ± 4.6	4.2 ± 2.4	0.89
FBF	−1.1 ± 9.1	7.3 ± 4.8*	0.75	2.6 ± 5.0	3.6 ± 4.2	0.86
MTfbf	2.6 ± 5.9	5.1 ± 3.6*	0.79	2.9 ± 4.6	3.9 ± 3.8	0.79
MT	−0.2 ± 7.0	5.0 ± 4.5*†	0.81	0.8 ± 3.6	2.8 ± 2.2	0.95
LMCfbf	0.6 ± 6.1	4.9 ± 3.3*	0.75	1.2 ± 3.3	2.7 ± 2.1	0.90

*Significantly different compared with raw data.
†Trend difference compared with FBF.

in Figure 7, or as occurs within a clinical scan (Fig. 2B). This may be accounted for by the different local environments of the 2 regions. For example, as the VS and DS ROIs move rostrally in the *z*-plane, either due to movement of the ROI rostrally or to the volunteer moving caudally, the activity in the DS is more profoundly reduced than the activity in the VS. This is because the ROIs are no longer sampling the VS and DS and are, instead, sampling other local brain regions. In this case, the VS ROI samples what is actually DS (a high-activity region). The DS ROI, in contrast, samples brain regions with low radioactivity and, hence, shows a sharp drop in activity. In practice, movements made by volunteers during scanning do not occur in only 1 plane at a time, making it very difficult to account for the different patterns of uptake observed in Figures 2B and 3, for example. It is equally difficult to account for the different effects the various methods of motion correction have on the time–activity curve in Figure 2B because subtle variations in the degree of realignment between methods have correspondingly subtle and unpredictable effects on the time–activity curve.

The use of head movement correction is likely to be beneficial for other radioligands with different patterns of uptake than ^{11}C-raclopride. ^{11}C-Raclopride provides a good exemplar of the method because its highly localized pattern of uptake in the striatum with very little uptake in neighboring regions makes BP measurements very vulnerable to effects of head movement. However, radioligands with cortical uptake may be similarly vulnerable because of the close proximity of scalp. Because the Polaris-based methods do not rely on the PET data to compensate for movements, they should be applicable to other radioligands, where they are likely to have similar benefits of improved accuracy and test–retest reliability.

The SPM analyses showed that in this set of raw data, BP tended to reduce in the anteroventral portion of the striatum and increase in the dorsal as well as ventral regions between scanning periods. After different methods of

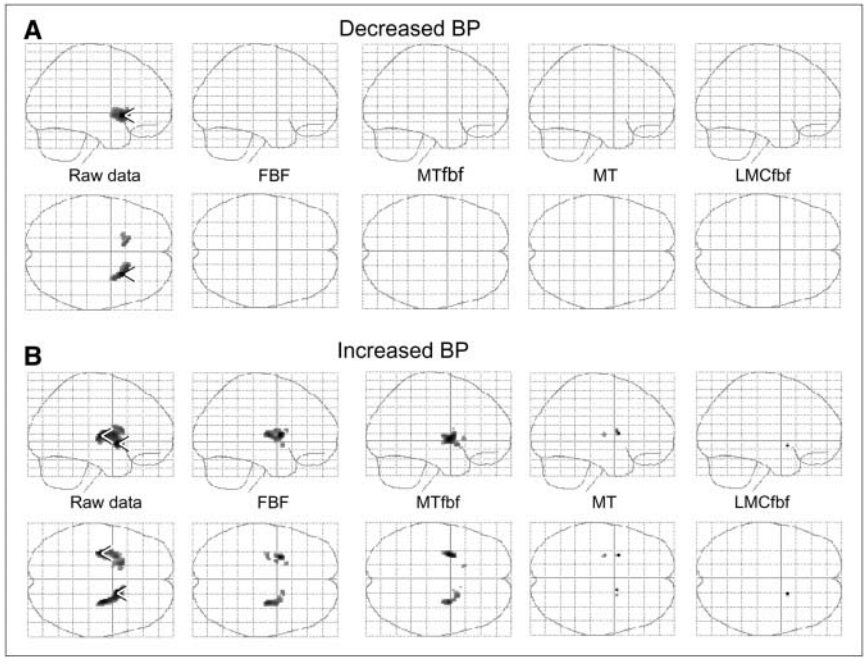

FIGURE 6. SPM comparisons of BP between first (A) and second (B) sampling periods. All voxels were significant at $P < 0.01$, uncorrected. Data are sagittal (top rows) and axial (bottom rows) glass brain views. Arrowheads indicate peak voxels in significant clusters.

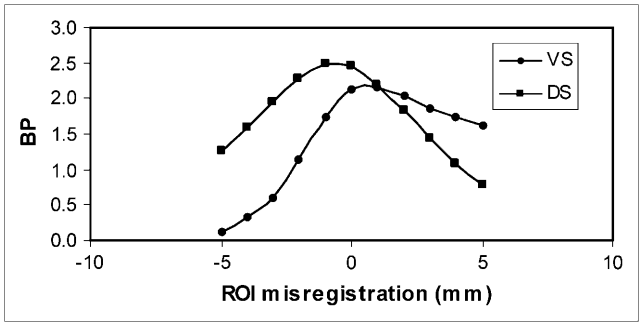

FIGURE 7. Measured BP in VS and DS ROI as ROI is moved a voxel at a time in the *z*-axis. Large changes in BP result from small changes in ROI position, demonstrating the susceptibility of measurements to movement.

movement correction, there were no voxels that significantly reduced in value between sample periods, although all methods continued to show voxels, which increased between the 2 periods (not corrected for multiple comparisons). It is likely that the different methods of head restraint used in different PET centers generate different patterns of apparent change in BP within the striatum (or, indeed, in extrastriatal regions), depending on the type of head movement they allow (*1,4*) and the regional distribution of the radioligand. A further factor that is likely to influence the type and degree of head movement volunteers make during a scan is the presence or absence of pharmacologic or behavioral stimulation during the scan. For example, agents such as amphetamines promote motor activity and may be anticipated to increase head movement. To date, the influence of such factors on PET and SPECT outcome measures has not been systematically evaluated. Few studies in the literature report whether scans have been rejected because of excessive head movement—perhaps because of the difficulty defining a cutoff point beyond which data are no longer reliable.

Changes in VS regional activity (percentage change in radioactivity per hour) showed a trend reduction by LMCfbf realignment compared with raw data and were significantly reduced compared with the FBF data by LMCfbf. The values in the DS are smaller than those previously reported (*5*). Mawlawi et al. (*5*) found that DS regions reduced in activity by $-12.9\% \pm 15.1\%$ and $-8.5\% \pm 13.5\%$ per hour in dorsal caudate and dorsal putamen, respectively—changes that differed significantly from zero (it is not clear if raw or motion-corrected data are reported). In the VS, changes did not differ from zero and were of a similar order ($-3.2\% \pm 13.9\%$) as those reported here. The only other equilibrium data reported in the literature are more difficult to compare with our data because the striatum is not subdivided (*25*). However, the values of $-1.8\% \pm 9\%$ for the striatum and $0.6\% \pm 12.6\%$ in the cerebellum are very similar to our data.

Noise was significantly higher in the second sampling period and in the smaller VS ROI. This was presumably due to radioactive decay causing poorer counting statistics in later frames and smaller ROI. In the second period noise was reduced significantly in all ROIs by LMCfbf, by MT in the cerebellum, and by MTfbf in the VS and DS. Polaris-based methods performed better than FBF in the VS (Fig. 4). To our knowledge, only one other group has published a similar analysis of ^{11}C-raclopride BI data (*5*). Their study used somewhat higher injected doses of radioactivity (470 ± 166 MBq); however, noise levels in the data presented here are comparable with the raw dataset and are better in the realigned data. Mawlawi et al. (*5*) also found that FBF realignment reduced noise levels.

Three different Polaris-guided methods are reported here. Two methods used list-mode repositioning (MT and LMCfbf), whereas the other method (MTfbf) used image repositioning. Neither the FBF (which does not use Polaris data) nor the MTfbf method can correct for movement within the frame. If no within-frame movement occurs, the MTfbf and LMCfbf images are identical. It is possible that both frame-based methods would have performed better if the frame duration had been shorter, but this has not been examined to date. If large movements occur with respect to the position during transmission scanning, the MT method suffers from 2 drawbacks compared with LMCfbf: First, the standard scatter estimation is no longer accurate, which will introduce a bias increasing with the amount of the movement. The reason for this, as explained by Thielemans (*15*), is that the scatter distribution after realignment of the LORs is not the same as the scatter distribution that would have been measured in the target position (target position is the motion-corrected position). Second, because of the requirement of 3DRP for consistent data, some of the measured data cannot be used (*14*), which will lead to an increase in noise for larger movements. Of these 2 effects, the first was illustrated by Thielemans (*15*), showing quantitative difficulties of MT on phantom data with fairly large movements. The effect may be responsible for the slightly reduced BP measured in the DS when MT is compared with other methods. The expected reduction in noise of LMCfbf over MT is reflected in the data of Figure 4.

Fulton et al. (*26*) have published a quantitative comparison between MT and MTfbf on phantom data. They found that the MT method provided somewhat better quantification than MTfbf, which was considerably better than using no motion correction. However, this article has a different implementation of MT compared with ours. In our method, each LOR is weighted after repositioning with a factor that takes its measurement time into account (and some LORs are filled in by forward projection), whereas Fulton et al. use a global factor (i.e., identical for every LOR). In our experience, such a global factor is not sufficient for accurate quantification for arbitrary movements. This might be partially explained by the fact that we have used the 3DRP reconstruction algorithm, whereas Fulton et al. used Fourier rebinning plus filtered backprojection.

Limitations

Because these data were acquired with the volunteers at rest, they are likely to have moved less than volunteers in a study where a pharmacologic agent is administered or where the paradigm under investigation requires a motor response (unpublished observations). However, Polaris-guided methods have been validated on phantom studies (*10,12–15*) with much larger degrees of movement than generally occur in clinical studies, suggesting that the technique should be useful in different study designs. Although there are clear theoretical differences between the different Polaris-guided methods, it was not possible to fully distinguish their relative effects on this dataset. It will be necessary to apply the methods to phantom studies with relatively large movements to provide a sufficient "challenge" to reveal relative advantages and disadvantages.

CONCLUSION

The use of a MT realignment system such as Polaris confers significant advantages to ^{11}C-raclopride PET studies, potentially allowing single-scan, dual-condition studies to detect small changes in radioligand binding in the VS with considerably increased statistical power compared with existing methods. Of the 3 Polaris-guided methods, LMCfbf is theoretically the most reliable.

ACKNOWLEDGMENTS

Support was received from the Wellcome Trust and from the Medical Research Council. We thank all volunteers for their time and gratefully acknowledge the technical support of the staff of Hammersmith Imanet.

REFERENCES

1. Green MV, Seidel J, Stein SD, et al. Head movement in normal subjects during simulated PET brain imaging with and without head restraint. *J Nucl Med.* 1994; 35:1538–1546.
2. Bergstrom M, Boethius J, Eriksson L, Greitz T, Ribbe T, Widen L. Head fixation device for reproducible position alignment in transmission CT and positron emission tomography. *J Comput Assist Tomogr.* 1981;5:136–141.
3. Beyer T, Tellmann L, Nickel I, Pietrzyk U. On the use of positioning aids to reduce misregistration in the head and neck in whole-body PET/CT studies. *J Nucl Med.* 2005;46:596–602.
4. Ruttimann UE, Andreason PJ, Rio D. Head motion during positron emission tomography: Is it significant? *Psychiatry Res.* 1995;61:43–51.
5. Mawlawi O, Martinez D, Slifstein M, et al. Imaging human mesolimbic dopamine transmission with positron emission tomography. I. Accuracy and precision of D_2 receptor parameter measurements in ventral striatum. *J Cereb Blood Flow Metab.* 2001;21:1034–1057.
6. Andersson JL, Vagnhammar BE, Schneider H. Accurate attenuation correction despite movement during PET imaging. *J Nucl Med.* 1995;36:670–678.
7. Dagher A, Gunn R, Lockwood G, Cunningham V, Grasby P, Brooks D. Measuring neurotransmitter release with PET: methodological issues. In: Carson R, Daube-Witherspoon M, Herscovitch P, eds. *Quantitative Functional Brain Imaging with Positron Emission Tomography.* Oxford, U.K.: Academic Press; 1998:449-454.
8. Menke M, Atkins M, Buckley K. Compensation methods for head motion detected during PET imaging. *IEEE Trans Nucl Sci.* 1996;43:310–317.
9. Picard Y, Thompson CJ. Motion correction of PET images using multiple acquisition frames. *IEEE Trans Med Imaging.* 1997;16:137–144.
10. Lopresti BJ, Russo A, Jones WF, et al. Implementation and performance of an optical motion tracking system for high resolution brain PET imaging. *Proceedings for the 1998 IEEE Nuclear Science Symposium: Medical Imaging Conference.* November 8–14, 1998. IEEE; 1999:1127–1131.
11. Hutton BF, Kyme AZ, Lau YH, Skerrett DW, Fulton RR. A hybrid 3-D reconstruction/registration algorithm for correction of head motion in emission tomography. *IEEE Trans Nucl Sci.* 2002;49:188–194.
12. Goldstein SR, Daube-Witherspoon M, Green MV, Eidsath A. A head motion measurement system suitable for emission computed tomography. *IEEE Trans Med Imaging.* 1997;16:17–27.
13. Bloomfield PM, Spinks TJ, Reed J, et al. The design and implementation of a motion correction scheme for neurological PET. *Phys Med Biol.* 2003;48: 959–978.
14. Thielemans K, Mustafovic S, Schnorr L. Image reconstruction of motion corrected sinograms. In: Scott, Metzler, eds. *Proceedings for the IEEE Medical Imaging Conference.* October 19–25, 2003. Vol 4. Portland, OR: IEEE; 2003:2401–2406.
15. Thielemans K. Scatter estimation and motion correction in PET. In: Yu B, ed. *Proceedings for the IEEE Medical Imaging Conference.* Fajardo, Puerto Rico: IEEE; 2005:1745–1747.
16. Herzog H, Tellmann L, Fulton R, et al. Motion artifact reduction on parametric PET images of neuroreceptor binding. *J Nucl Med.* 2005;46:1059–1065.
17. Watabe H, Endres CJ, Breier A, Schmall B, Eckelman WC, Carson RE. Measurement of dopamine release with continuous infusion of [^{11}C]raclopride: optimization and signal-to-noise considerations. *J Nucl Med.* 2000;41:522–530.
18. Spinks TJ, Jones T, Bloomfield PM, et al. Physical characteristics of the ECAT EXACT 3D positron tomograph. *Phys Med Biol.* 2000;45:2601–2618.
19. Kinahan PE, Rogers JG. Analytic 3D image reconstruction using all detected events. *IEEE Trans Nucl Sci.* 1989;36:964–968.
20. Meyer JH, Gunn RN, Myers R, Grasby PM. Assessment of spatial normalization of PET ligand images using ligand-specific templates. *Neuroimage.* 1999;9: 545–553.
21. Ashburner J, Friston K. Non-linear spatial normalisation using basis functions. *Hum Brain Mapp.* 1999;7:254–266.
22. Battle G. A block spin construction of ondelettes:1. Lemarie functions. *Commun Math Phys.* 1987;7:601–615.
23. Turkheimer FE, Brett M, Visvikis D, Cunningham VJ. Multiresolution analysis of emission tomography images in the wavelet domain. *J Cereb Blood Flow Metab.* 1999;19:1189–1208.
24. Studholme C, Hill DL, Hawkes DJ. Automated three-dimensional registration of magnetic resonance and positron emission tomography brain images by multiresolution optimization of voxel similarity measures. *Med Phys.* 1997; 24:25–35.
25. Carson RE, Breier A, de Bartolomeis A, et al. Quantification of amphetamine-induced changes in [^{11}C]raclopride binding with continuous infusion. *J Cereb Blood Flow Metab.* 1997;17:437–447.
26. Fulton R, Tellmann L, Pietrzyk U, et al. Accuracy of motion correction methods for PET brain imaging. *IEEE Med Imaging.* 2004;7:4226–4230.